Morphology of Nested Fullerenes

D. J. Srolovitz,* S. A. Safran, M. Homyonfer, and R. Tenne
Department of Materials and Interfaces, Weizmann Institute of Science, Rehovot 76100, Israel
(Received 9 August 1994; revised manuscript received 15 December 1994)

We introduce a continuum model which shows that dislocations and/or grain boundaries are intrinsic features of nested fullerenes whose thickness exceeds a critical value to relieve the large inherent strains in these structures. The ratio of the thickness to the radius of the nested fullerenes is determined by the ratio of the surface to curvature and dislocation (or grain boundary) energies. Confirming experimental evidence is presented for nested fullerenes with small thicknesses and with spherosymmetric shapes.

PACS numbers: 61.46.+w, 61.50.Jr, 61.72.–y

Recent experimental and theoretical work [1–3] suggest that carbon-based, nested fullerenes (also known as onion skin, multilayered, or Russian doll fullerenes) are more stable than single shell fullerenes when the number of carbon atoms exceeds a critical size N_c ($N_c > 10^3$ [2,3]). Nested fullerenelike structures have also been observed in several layered metal dichalcogenides [4] MX_2, where M = W, Mo and X = S, Se. In the present Letter, we employ a continuum elastic theory to demonstrate that either dislocations or grain boundaries are an intrinsic component of thick walled, nested fullerenes. We present experimental evidence, consistent with this picture, which shows that nested fullerenes with small thickness show a spherosymmetric shape while thick, nested fullerenes show either faceted or nonfaceted shapes associated with grain boundary or dislocation relaxed structures.

The importance of dislocations can be seen by considering a two-shell, spherical graphitic fullerene where geometry dictates that the outer shell contains more atoms than the inner shell. These two shells cannot pack together perfectly like the (0002) planes in graphite. While locally the layer packing may be similar to graphite, the regions of good lattice match must be separated by discommensurations or, equivalently, dislocations. Hence any discussion of the energetics must include these geometrically necessary defects. While atomistic methods [2,3,5–10] have proven useful in determining the energetics of competing fullerene structures, such approaches are less useful for nested structures with large numbers of atoms [1], where our continuum approach is most applicable.

The energy of a nested fullerene has three main components: the curvature or bending elastic energy, the defect energy, and the surface energy. The elastic energy W_u associated with bending a defect-free film of thickness d about two orthogonal axes is [11,12]

$$W_u = \frac{d^3}{12}(2kH^2 + \bar{k}K), \tag{1}$$

where $H = (\kappa_1 + \kappa_2)/2$ is the mean curvature, $K = \kappa_1\kappa_2$ is the Gaussian curvature, and κ_1 and κ_2 are the two principle curvatures. The bending moduli k and $\bar{k}$ are functions of the elastic constants, C_{ij} of the material: $k = C_{11} - C_{13}^2/C_{33} = E/(1 - \sigma^2)$ is a measure of the resistance of the system to bending with a nonzero mean curvature, while the saddle-splay modulus $\bar{k} = -2C_{66} = -E/(1 + \sigma)$ is a measure of the energy cost for making saddle-type structures. These anisotropic elastic expressions for k and $\bar{k}$ are given for the case of hexagonal symmetry, where the c axis is normal to the film surface [11,13]. E and σ are isotropic elastic constants—Young's modulus and Poisson ratio, respectively. For a sphere of radius $R = 1/\kappa$ (R is the distance from the center to the middle of the spherical shell), this reduces to $W_u = \chi d^3\kappa^2/12$, where $\chi = 2k + \bar{k}$. This expression assumes that the whole thin film bends coherently. However, if the atomic planes can slip without resistance, the elastic energy is relaxed to $W_r = \chi dc^2\kappa^2/12$, where c is the spacing between atomic layers. This energy is simply the energy W_u to independently bend d/c layers of thickness c.

When the crystal planes in a thin film slip relative to each other, the crystal structure is disrupted. When this slippage is localized in the form of dislocations, rather than continuously distributed, the crystal structure is disrupted less and this slippage is energetically less costly. In a thin film geometry, the energy of a dislocation (per unit length) may be approximated as $W_\perp \approx (Jb^2/4\pi)\ln(R_0/r_0)$, where b is the Burgers vector (strength) of the dislocation, and r_0 is the (atomic scale) inner cutoff radius. For simplicity, we shall set $b = c$, the atomic size. The outer cutoff radius R_0 is approximately equal to half the spacing between dislocations or the film thickness, whichever is smaller. $J = E/[2(1 - \sigma^2)]$ in an isotropic solid and $J \approx (C_{11}C_{55})^{1/2}$ in a layered material [13,14]. This dislocation energy omits the relatively small contribution of dislocation [14] and disclination (see below) [5] cores at large system sizes.

The total elastic energy E_b associated with bending a thin film into a spherical shell of thickness d and radius $R = 1/\kappa$, includes both the bending energy and the dislocation energy. We define the dimensionless thickness $h = d/c$, radius $r = R/c$, and $\nu = V/c^3$. The volume of the thin spherical shell is $V \approx 4\pi R^2 d$. Minimizing this

energy with respect to dislocation density yields [13,15]

$$E_b = \begin{cases} B_0 h^3, & \kappa < \kappa_c, \\ B_1 h + B_2\sqrt{\nu h} - B_3 \nu/h^2, & \kappa > \kappa_c, \end{cases} \quad (2)$$

where $B_0 = \pi\chi c^3/3$, $B_1 = B_0$, $B_2 = B_0\beta J/(\chi\pi^{1/2})$, $B_3 = B_0(\beta J)^2/(4\pi\chi^2)$, $\alpha = 1 - 1/h^2$, and $\beta = [3/(\pi\alpha)]\ln(R_0/r_0)$, and the critical curvature is defined by $\kappa_c = \beta J/(\chi h^2 c)$ [13]. In the derivation of Eq. (2), we assumed that although the shell is thin compared to the radius $h/r \ll 1$, it is thick compared to an atomic spacing $h \gg 1$, and terms of higher order than linear in h/r are neglected. For $\kappa < \kappa_c$, the total elastic energies of nested fullerenes are lower when they are bent coherently (without dislocations). However, for $\kappa > \kappa_c$, the elastic energy is lowered by forming a dislocation array of constant density. Therefore, a phase transition between undislocated and dislocated, nested fullerenes occur at a finite, critical curvature κ_c, which is dependent on the elastic constant of the material and is inversely proportional to the square of the thickness. For a fixed curvature, one can think of a critical thickness below which the layers bend with no dislocations and above which the structure contains dislocations. The theory shows that thin, nested fullerenes have high critical curvatures and one might expect them to grow relatively dislocation free. The same analysis and conclusions apply to the formation of grain boundaries or polygonalized morphologies; dislocations tend to organize themselves into grain boundaries and theory [13] predicts that thin, nested fullerenes would tend to be grain boundary free and show spherically symmetric morphologies.

In addition to the bulk terms, the total energy of a nested fullerene also includes contributions from the inner and outer surfaces of the spherical shell. In all known nested fullerenes, the bonding within the atomic layers (i.e., the basal planes) is covalent, while that between layers is primarily due to van der Waals forces. Therefore, the surface energy can be written $E_s = S\nu/h$, where $S = 2\gamma c^2$ and γ is the surface energy (per unit area) of a semi-infinite solid of the film material and related to the van der Waals energies.

The total energy of the nested fullerene is $E_{\text{tot}} = E_s + E_b$. The equilibrium nested fullerene thickness may be obtained by minimizing E_{tot} with respect to h at fixed ν. The balance between the h^3 and $1/h$ terms determine the equilibrium aspect ratio $\eta = h/r = d/R$ for $\kappa < \kappa_c$. The large ν limit, the competition between the terms proportional to $h^{1/2}$ and $1/h$ determine η_{eq}, when $\kappa > \kappa_c$. For large ν, the equilibrium aspect ratio η_{eq} is

$$\eta_{\text{eq}} \approx \begin{cases} (2\sqrt{\pi}/3^{3/8})(S^3/B_0^3\nu)^{1/8}, & \kappa < \kappa_c, \\ (4\sqrt{\pi})(S/B_2), & \kappa > \kappa_c, \end{cases} \quad (3)$$

Equation (3) suggests that the equilibrium thickness to radius ratio of nested fullerenes should decrease slowly with an increasing number of atoms when $\kappa < \kappa_c$, i.e., small curvature and/or thickness. On the other hand, when $\kappa > \kappa_c$ (large curvature and/or thickness), η_{eq} is constant to leading order in ν, and is determined by the surface energy to relaxed bending energy ratio.

The equilibrium shape of nested fullerenes predicted by Eq. (3) is evaluated using the accurately known elastic constants [16] of graphite; the uncertainty in the (0001) surface energy is of the order of 50% [17]. In MoS_2, the elastic constants are also known [18], but the uncertainty in the (0001) surface energy is of the order of a factor of 10 [19,20]. Using the available data, we estimate that the equilibrium aspect ratio is $\eta = 0.06$ for the graphitic, nested fullerene and $\eta = 0.1$ for MoS_2, assuming that $\kappa > \kappa_c$. The qualitative message is that *equilibrium* large scale fullerenes should be "thin," i.e., they should have a small thickness to radius ratio.

Similar considerations can be used to analyze the energies of polygonalized, nested fullerenes, where the polygonalization is treated in terms of grain boundaries. Speck [21] was the first to compare the energetic's spherical and faceted carbon layers in a study of carbon blacks, but did not consider the important effects of dislocations or anisotropy or determine the equilibrium value of η which are included in the present analysis. The energy associated with the grain boundaries in a nested fullerene is equal to the grain boundary energy per unit area γ_{gb} times the total grain boundary area. The grain boundary area is proportional to h and the total length of all edges, which is proportional to R. The proportionality constant ξ depends on the type of polyhedron and typically decreases slowly with an increasing number of faces for fixed volume. The total energy of a faceted, nested fullerene has contributions from both the grain boundary energy ($E_{\text{gb}} = \gamma_{\text{gb}} hR\xi$) and the energies of the inner and outer surfaces. Following the same procedure used to determine the total energy of dislocated, nested fullerenes, we find $E_{\text{tot}}^{\text{gb}} = G\sqrt{\nu h} + S\nu/h$ for $\kappa > \kappa_c^{\text{gb}}$, where $G = \xi\gamma_{\text{gb}} c^2/\sqrt{4\pi}$ and κ_c^{gb} are the critical curvature for forming grain boundaries. In isotropic materials, $\kappa_c^{\text{gb}} < \kappa_c$ [13]. For $\kappa < \kappa_c^{\text{gb}}$, the energy is as given in Eq. (2). $E_{\text{tot}}^{\text{gb}}$ exhibits a minimum at $\eta_{\text{eq}}^{\text{gb}} = h/r = d/R = 4\sqrt{\pi}S/G$. Therefore, $\eta_{\text{eq}}^{\text{gb}}$ is independent of the number of atoms ν in the large ν limit and is determined by the ratio of the surface to the relaxed bending energies.

Comparison of $\eta_{\text{eq}}^{\text{gb}}$ with η_{eq}, shows that the η_{eq} for the two relaxation mechanisms are both independent of ν and proportional to the surface energy S. The ratio $\eta_{\text{eq}}^{\text{gb}}/\eta_{\text{eq}} \approx [2cJ\ln(R_0/r_0)]/(\xi\gamma_{\text{gb}}\alpha)$ is approximately 5 for graphite. The uncertainty in this value of $\eta_{\text{eq}}^{\text{gb}}$ is of the same order as that for η_{eq}, owing to the uncertainty in the grain boundary energy. This value of the ratio is based upon the assumption that the polyhedral, nested fullerene is icosahedral such that $\xi \approx 20$, $J = 6.5 \times 10^{10}$ Pa, $\gamma_{\text{gb}} = 1$ J/m^2, $\alpha = 1$, $c = 2 \times 10^{-10}$ m, and $\ln(R_0/r_0) = 5$. In any case, we expect that $\eta_{\text{eq}}^{\text{gb}} > \eta_{\text{eq}}$, since the dislocation energy is typically lowered when they organize into grain boundaries. This would also suggest that polyhedral

(faceted), nested fullerenes should have lower energy than those relaxed by dislocations (for the same ν). However, since there are no topological constraints on the number of grain boundaries and the grain boundary energy changes rapidly with misorientation at small angles, it is possible for dislocation relaxation to lead to lower energy structures as compared with structures with many low-angle grain boundaries. The rearrangement of dislocations into a relatively small number of high misorientation grain boundaries may be limited by kinetics.

One obvious difficulty in experimentally determining η is the necessity to distinguish between shapes determined by growth and/or kinetic factors and true equilibrium shapes. Clearly, if the nested fullerenes grow in a layer-by-layer mode, then it is unlikely that the resultant structures are in equilibrium. Carbon, nested fullerenes are typically found to have interior radii very close to that of C_{60}, while the outer radii vary over a substantial range [22]. Nested fullerenes of MoS_2, on the other hand, can show a wide range of both inner and outer radii (see Fig. 1). Typical MoS_2, nested fullerene, produced from the sulfidation of a very thin film of metal oxide on a quartz substrate, is shown in the atomic resolution electron micrograph in Figs. 1(a) and 1(b). Examination of the nearly spherical, nested fullerene in Fig. 1(a) shows that such structures may be described in terms of a relatively large number of low-angle grain boundaries or by a uniform array of dislocations. The fullerene in Fig. 1(b) is strongly faceted, with very flat atomic planes meeting at sharply defined grain boundaries. We note that both of these samples are grown under conditions which are far from equilibrium and comparison with the theory is not possible.

Recently, however, a new technique for the gas phase synthesis of MoS_2, nested fullerenes has been developed [23,24]. In this technique, which affords a much better control over the growth conditions than the previous gas-solid synthetic route [4], gaseous MoO_{3-x} and H_2S gases diluted in a carrier gas are reacted at elevated temperatures (>800 °C). It is expected that, in this synthetic route, the nested fullerenes grow independently of each other, mostly through interaction with the carrier (forming) gas and hence growth conditions which are closer to equilibrium prevail. Copious amounts of the nested fullerene and nanotube phases are obtained in this way.

It appears that even in this synthesis the role of the substrate, on which the nested fullerenes are being collected, cannot be overlooked [23,24]. If a NbS_2 substrate is used, large amounts of nested fullerenes consisting of two shells and of various shapes are observed. A typical example of a nested fullerene with $\eta = 0.2$ and a nearly spherical shape is shown in Fig. 1(c). Most of the nested fullerenes produced in this way exhibit values of $\eta \leq 0.2$, the majority of these are at least partially faceted—containing at least one grain boundary. In other

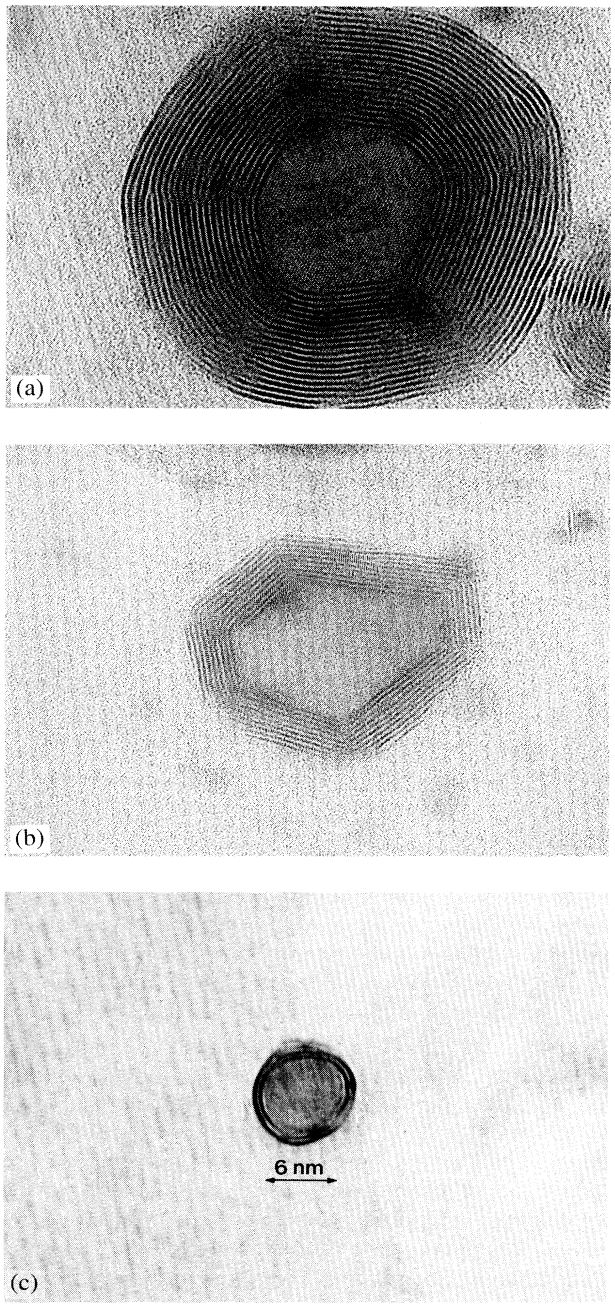

FIG. 1. High resolution transmission electron microscope image of MoS_2 fullerenes. The distance between the fringes is 0.62 nm, which is half of the c-axis lattice constant in hexagonal MoS_2. (a) and (b) show nested MoS_2 fullerenes prepared by firing a 10 nm film of MoO_3 in H_2S under reducing conditions (see [4] for more details) with (a) a nearly spherical shape and (b) a polyhedral, faceted shape, respectively. (c) shows a nearly spherical, two-layer, nested fullerene produced in a gas phase reaction between a stream of gaseous molybdenum suboxide and H_2S diluted in a carrier gas of H_2/N_2 (5%/95%).

cases, where amorphous carbon has been used as a substrate, single-layer nonfaceted fullerenes with a spherosymmetric shape were recently obtained [24]. In another reactor of different design with a quartz substrate as a collector [23], values of η closer to 0.7 were typically obtained. It is very likely that under the harsh flow conditions in this reactor, the lighter, nested fullerenes (with $\eta = 0.1-0.2$) are swept away by the gas flow and are collected on some other parts of the reactor farther upstream from the substrate. Thus, although a conclusive comparison between theory and experiment cannot be made at this time, we now have experimental evidence that large quantities of nested fullerenes with η as small as 0.1 do occur. These experimental results are in agreement with our theoretical predictions presented above.

The HRTEM micrographs were prepared in collaboration with Dr. J. L. Hutchinson and Dr. L. Margulis. D.I.S. gratefully acknowledges the hospitality of The Weizmann Institute of Science and the support of the Division of Materials Science of the U.S. Department of Energy (Grant No. FG02-88ER-45367). S.A.S. is grateful for the support of the Donors of the Petroleum Research Fund, administered by the ACS and the Israel Academy of Sciences. M. H. and R. T.'s research was sponsored by the US-Israel Binational Science Foundation and the Manof project of the Israeli Ministry of Science and Arts.

*Permanent address: Dept. of Materials Science and Engineering, University of Michigan, Ann Arbor, MI 41809-2136.

[1] D. Ugarte, Europhys. Lett. **22**, 45 (1993); Nature (London) **359**, 707 (1992).
[2] A. Maiti, C. J. Brabec, and J. Bernholc, Phys. Rev. Lett. **70**, 3023 (1993).
[3] J. P. Lu and W. Yang, Phys. Rev. B **49**, 11 421 (1994).
[4] R. Tenne, L. Margulis, M. Genut, and G. Hodes, Nature (London) **360**, 444 (1992); L. Margulis, G. Salitra, M. Talianker, and R. Tenne, Nature (London) **365**, 113 (1993); M. Hershfinkel, L. A. Gheber, V. Volterra, J. L. Hutchinson, L. Margulis, and R. Tenne, J. Am. Chem. Soc. **116**, 1914 (1994).
[5] J. Tersoff, Phys. Rev. B **46**, 15 546 (1992).
[6] G. B. Adams, O. F. Sankey, J. B. Page, M. O'Keeffe, and D. A. Drabold, Science **256**, 1792 (1992).
[7] Q.-M. Zhang, J.-Y. Yi, and J. Bernholc, Phys. Rev. Lett. **66**, 2633 (1991).
[8] B. L. Zhang, C. H. Xu, C. Z. Wang, C. T. Chan, and K. M. Ho, Phys. Rev. B **46**, 7333 (1992).
[9] D. Tomanek and M. A. Schluter, Phys. Rev. Lett. **67**, 2331 (1991).
[10] P. Ballone and P. Milani, Phys. Rev. B **42**, 3201 (1990).
[11] L. D. Landau and E. M. Lifshitz, *Theory of Elasticity* (Pergamon, Oxford, 1986), 3rd ed.
[12] W. Helfrich, Z. Naturforsch. **28c**, 693 (1973).
[13] D. J. Srolovitz, S. A. Safran, and R. Tenne, Phys. Rev. E **49**, 5260 (1994).
[14] J. P. Hirth and J. Lothe, *Theory of Dislocations* (John Wiley, New York, 1982).
[15] Tersoff [5] showed that for a single layer of curved graphite, the bending energy has logarithmic corrections (i.e., $\log R$) attributable to the disclinations that must be present in order to fold a sheet into a closed, curved shape. This generates additional logarithmic terms in Eq. (2) which rescale the constants in this equation but are much less important than the algebraic terms in determining the morphology.
[16] O. L. Blakeslee, D. G. Proctor, E. J. Seldin, G. B. Spence, and T. Weng, J. Appl. Phys. **41**, 3373 (1970).
[17] J. Abrahamson, Carbon **11**, 337 (1973).
[18] J. L. Feldman, J. Phys. Chem. Solids **37**, 1141 (1976).
[19] M. A. Berding, S. Krishnamurthy, A. Sher, and A.-B. Chen, J. Appl. Phys. **67**, 6175 (1990).
[20] A. I. Brudnyi and A. F. Karmadonov, Wear **33**, 243 (1975).
[21] J. S. Speck, J. Appl. Phys. **67**, 495 (1990).
[22] S. Iijima, J. Cryst. Growth **50**, 675 (1980).
[23] Y. Feldmann, E. Wasserman, D. Srolovitz, and R. Tenne, Science (to be published).
[24] M. Homyonfer and R. Tenne (to be published).

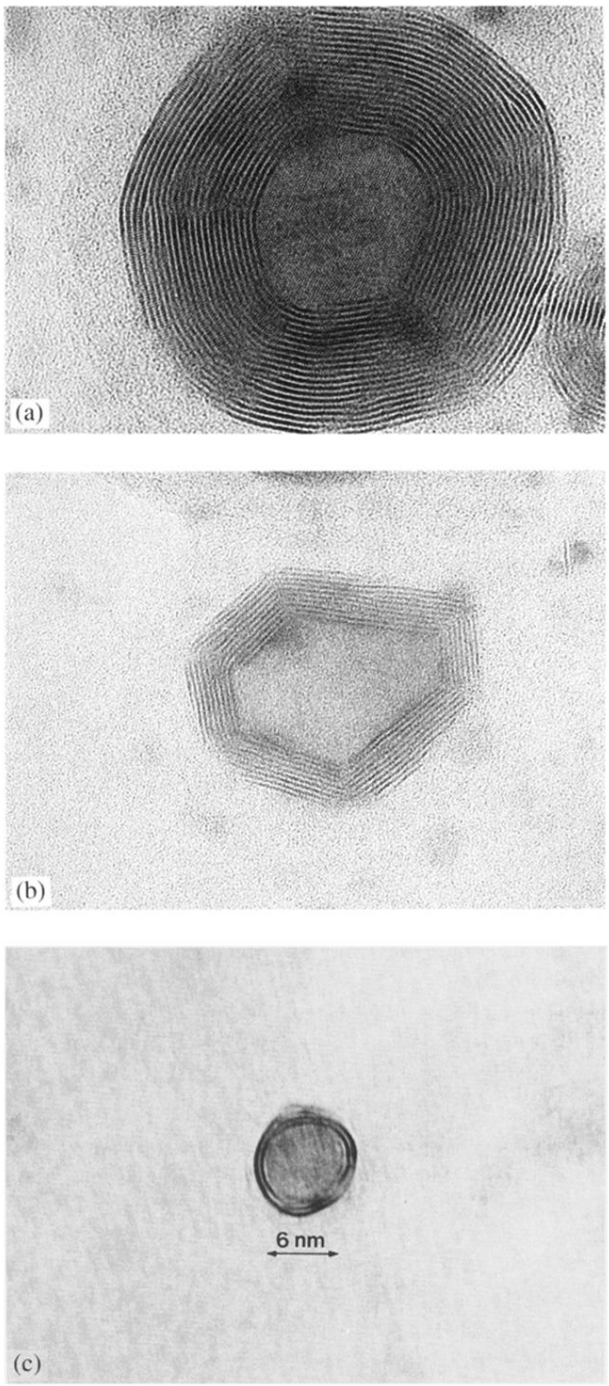

FIG. 1. High resolution transmission electron microscope image of MoS_2 fullerenes. The distance between the fringes is 0.62 nm, which is half of the *c*-axis lattice constant in hexagonal MoS_2. (a) and (b) show nested MoS_2 fullerenes prepared by firing a 10 nm film of MoO_3 in H_2S under reducing conditions (see [4] for more details) with (a) a nearly spherical shape and (b) a polyhedral, faceted shape, respectively. (c) shows a nearly spherical, two-layer, nested fullerene produced in a gas phase reaction between a stream of gaseous molybdenum suboxide and H_2S diluted in a carrier gas of H_2/N_2 (5%/95%).